Office of Naval Research
Contract N00014-89-J-1276
Technical Report No. UWA/DME/TR-89/62

J-Resistance Curves of Aluminum Specimens Using Moire Interferometry

by

B. S.-J. Kang, M.S. Dadkhah and A.S. Kobayashi

April 1989

The research reported in this technical report was made possible through support extended to the Department of Mechanical Engineering, University of Washington, by the Office of Naval Research under Contract N00014-89-J-1276. Reproduction in whole or in part is permitted for any purpose of the United States Government.

J-Resistance Curves of Aluminum Specimens Using Moire Interferometry

B. S.-J. Kang*, M.S. Dadkhah** and A.S. Kobayashi***

ABSTRACT

Errors involved in using the approximate J-evaluation procedure are evaluated by comparing the resistance curves of large 2024-O and 5052-H32 aluminum, single-edge cracked, cruciform specimens under uniaxial and biaxial loadings with those obtained by an exact procedure. This comparative study shows that under uniaxial loading, the J-resistance curves obtained by the approximate procedure are within six percent of those obtained by the exact procedure. For the biaxial loading, however, the difference is about eighteen percent. The specimen size and geometry dependence of the J-resistance curves of 2024-O and 5052-H32 aluminum specimens are also discussed.

INTRODUCTION

At present, most elastic-plastic fracture mechanics (EPFM) methodologies are based on the J-integral or the crack opening displacement (COD) approach. The J-resistance curve (J_R curve) approach in particular has been popular for evaluating elastic-plastic stable crack growth and ductile fracture of high toughness materials, such as A533B steel [1], and 2219-T87 aluminum [2]. Questions have been raised, however, regarding the specimen size and geometry dependence of the J-resistance curve [3,4,5], i.e. the use of J-resistance curve obtained by small laboratory specimens for predicting elastic-plastic crack growth resistance in large engineering structures.

Several experimental methods have been proposed for determining the J-Δa (J_R) curve. Generally the J values are determined from the measured far-field load versus load-line displacement curve and the amount of crack

* Assistant Professor, Department of Mechanical and Aerospace Engineering, West Virginia University, Morgantown, WV 26506

** Research Scientist, Science Center, Rockwell International Corp., Thousand Oaks, CA 91360.

*** Professor, Department of Mechanical Engineering, University of Washington, Seattle, WA 98195.

growth, Δa, is determined by such methods as the unloading compliance method [6], the electric potential method [7], the key curve method [8] and the ultrasonic method [9]. In contrast to these far-field methods, the authors have presented an approximate [10.11] and an exact [12] procedures for determining the J-integral values based on the displacement fields obtained by moire interferometry. These two procedures are based on the original J-integral definition for evaluating the J values along a contour either the near, middle or far crack-tip fields, such as those shown in Figs. 1 and 2. The purpose of this paper is to assess the accuracy of the J values evaluated by the simple and convenient approximate procedure through a comparative study with those values obtained by the exact procedure. We then extend the analysis to the discussion of the size and specimen dependence of the J-based resistance curves of 2024-O and 5052-H32 aluminum specimens under uniaxial and biaxial loadings.

ASSESSMENT OF THE APPROXIMATE J-EVALUATION PROCEDURE

The approximate J-evaluation procedure [10] is based on the assumption that two-dimensional states of stress and strain in a fracture specimen can be approximated by the uniaxial states of stress and strains. The uniaxial state can be determined by using only the u_y-displacement field obtained by the moire interferometry. This simplification is theoretically correct when the integration contour is taken along a far field location, i.e. the edges, of a single-edge-notched (SEN) specimen shown in Fig. 1. As for J-evaluation along a near crack tip contour (also shown in Fig. 1), a sensitivity study [10] showed that the approximate J-evaluation procedure incurred a fourteen percent error in the elastic crack-tip stress field and decreased to less than one percent in the HRR field [13,14].

In this paper, we present further application of the approximate J-evaluation procedure in large 2024-O and 5052-H32 aluminum single-edge cracked, cruciform specimens which were subjected to uniaxial and biaxial loadings. The moire interferometry tests were conducted by the second author who developed an exact J-evaluation procedure [12,15] which utilize both u_x and u_y moire displacement fields. Here, we apply the approximate J-evaluation procedure to the same u_y moire fringe patterns and compare these results to those obtained by the exact J-evaluation procedure. Material properties of the specimens are shown in Table 1.

RESULTS

Accuracy Assessment

Near- and far-field J values were evaluated by both procedures. Figures 3 and 4 show typical moire interferometry patterns corresponding to the u_y displacement field in an uniaxially loaded 5052-H32 and an biaxially loaded 2024-O aluminum cruciform specimens. The J values evaluated by the approximate and the exact J-evaluation procedures are listed in Tables 2, 3 and 4. These results show that the J values, which were obtained by the approximate procedure, are within six percent of those obtained by the exact procedure for uniaxially loaded cruciform specimens. However, the difference is about twenty percent for those under biaxial loading. This discrepancy is due to the region of large biaxial state of stress which invalidates the assumption of a dominant uniaxial state for the simplified approximation procedure.

Geometry Dependence of J-Δa Resistance Curve

Having proved the accuracy of the approximate J-evaluation procedure, previous J_R curves generated for small single edge notched (SEN) specimens using the approximate procedure can thus be used in a comparative study with those generated by the large cruciform specimens. Figure 5 shows superposed plots of the J-Δa curves for small 2024-O aluminum SEN specimens and large single-edge cracked cruciform specimens [11,15]. For the limited amount of crack growth considered in this study, the results indicate that the J_R curve is specimen size and geometry independent. This conclusion is reinforced by similar superposed plots of the COD and the CTOD resistance curves shown in Figs. 6 and 7. Figure 8 shows superposed plots of the J-Δa curves for small SEN and large 5052-H32 aluminum cruciform specimens. As shown in Fig. 8, the J_R curves start to deviate after about 0.6 mm of crack extension. Figure 9 shows superposed plots of the corresponding COD resistance curves. Similar deviation in the two curves after crack extension of 0.6 mm is observed.

DISCUSSION

The advantages of the approximate J-estimation procedure, which utilize a simplified contour integration based solely on the the dominant u_y

displacement field, are; i) simpler optics in the moire interferometry setup, and ii) the associated reduction in the data evaluation effort. Results of the comparative study of the J values obtained by the approximate and exact J-evaluation procedures indicate, however, that the approximate procedure can be used without incurring large errors only under uniaxial loading.

In the following, the specimen size and geometry dependence of the J-based resistance curves of 2024-O and 5052-H32 aluminum specimens are discussed.

J-Controlled Crack Growth

The base for the J-resistance curve approach for stable crack growth is the condition of J-controlled crack growth. Under such condition, nearly proportional loading must exist at the crack tip region and the amount of crack growth must be small compared to the region dominated by the HRR fields [13,14]. Within the condition of J-controlled crack growth, the J-integral and the related dJ/da are meaningful parameters for characterizing the crack growth [16,17]. Also, within the range of J-controlled crack growth, the J-resistance curve is unique and independent of the specimen size and geometry. Uncertainties arise as how to define the maximum range of crack extension for J-controlled crack growth [3]. Shih et.al [1] proposed that crack growth be limited to six percent of the ligament to ensure J-controlled crack growth. Recent studies [18] of J_R curves calculated using ASTM E1152, however, showed no specimen size dependence under large crack extension far in excess of the ASTM standard. In our previous studies based on the moire interferometry data [10,11,19], a J-dominated region was found in 2024-O aluminum specimens (a strain hardening material, see Table 1) and did not exist in 5052-H32 aluminum specimens (a nonhardening material, see Table 1). Figure 5 shows that for strain hardening material such as 2024-O aluminum of the same specimen thickness, the J_R curve is independent of the specimen size and geometry for crack extension at least up to 1 mm. For low strain hardening material, such as 5052-H32 aluminum, Figure 8 shows that the J_R curves deviate after 0.6 mm crack extension in this nonhardening material where the J-dominated zone shrinks to zero [20,21]. Thus some amount of strain hardening is essential for a valid J_R curve, which can be used to characterize ductile stable crack growth, to exist.

CONCLUSIONS

1. The errors involved in using the approximate J-evaluation procedure in large 2024-O and 5052-H32 aluminum, single-edge cracked, cruciform specimens under uniaxial and biaxial loadings are evaluated by comparing these results with those obtained by an exact procedure. This comparative study shows that under uniaxial loading, the J-integral values obtained by the approximate procedure are within six percent of those obtained by the exact procedure. For the biaxial loading, however, the difference is about eighteen percent.

2. Specimen size and geometry dependence of the J_R curves of 2024-O and 5052-H32 aluminum specimens are discussed. For 2024-O aluminum specimens of the same thickness, the J_R curve is independent of the specimen size and geometry for crack growth at least up to 1 mm. For 5052-H32 aluminum, however, the J_R curves deviate after 0.6 mm crack growth. These results suggest that some amount of strain hardening is necessary to ensure a specimen size and geometry independent J_R curve for characterizing ductile stable crack growth.

ACKNOWLEDGEMENTS

The work reported here was supported under ONR Contract N00014-89-J-1276. The authors acknowledge the support and encouragement of Dr. Yapa Rajapakse, ONR, during the course of this investigation. The first author also appreciates the support by the Mechanical and Aerospace Engineering Department, West Virginia University.

REFERENCES

1. C.F. Shih, H.G. deLorenzi, and W.R. Andrews, "Studies on Crack Initiation and Stable Crack Growth," Elastic-Plastic Fracture, ASTM STP 668, American Society for Testing and Materials, Philadelphia, Pa., pp.65-120, (1979).

2. M.F. Kanninen, G.T.Hahn, D.Broek, R.B.Stonesifer, C.W. Marschall, I.S. Abou-Sayed, and A. Zahoor, "Development of a Plastic Fracture Methodology," EPRI NP-1734, Project 601-1, Final Report, Electric Power Research Institute, March (1981).

3. M.R. Etemad and C.E. Turner, "Unique Elastic-Plastic R-Curves: Fact or Friction?" ASTM, 21st National Symposium on Fracture Mechanics, Annapolis, MD, June (1988).

4. H.A. Ernst, "Material Resistance and Instability Beyond J-Controlled Crack Growth," Elastic-Plastic Fracture: Second Symposium, Vol. 1 - Inelastic Crack Analysis, ASTM STP 803, American Society for Testing and Materials, Philadelphia, Pa., pp.I-191-I-214, (1983).

5. J.R. Rice, W.J. Drugan, and T.L. Sham, "Elastic-Plastic Analysis of Growing Cracks," Fracture Mechanics: Twelfth Conference, ASTM STP 700, American Society for Testing and Materials, Philadelphia, Pa., pp. 189-221, (1980).

6. J. D. Landes and D. E. McCabe, "Experimental Methods for Post-yield Fracture Toughness Determinations," Elastic-Plastic Fracture Mechanics, C.E. Turner Editor, pp.223-284, (1984).

7. G.M. Wilkowski, "Elastic-Plastic Fracture Studies Using the DC-EP Method," Ductile Fracture Test Method, Proceedings of a CSNI Workshop, Paris, pp.63-74, (1982).

8. Advances in Elastic-Plastic Fracture Analysis, EPRI NP-3607, Project 1237-1, Final Report, Electric Power Research Institute, August (1984).

9. Underwood, J.H. et.al., "End-on Ultrasonic Crack Measurements in Steel Fracture Toughness Specimens and Thick-wall Cylinders," The Detection and Measurement of Cracks, The Welding Institute, Cambridge, England, pp.31-39, (1976).

10. B.S.-J. Kang, A.S. Kobayashi, and D. Post, "Stable Crack Growth in Aluminum Tensile Specimens," Experimental Mechanics, 27(3), pp.234-245, (1987).

11. B.S.-J. Kang and A.S. Kobayashi, "J-Estimation Procedure Based on Moire Interferometry Data," ASME, Journal of Pressure Vessel Technology, 110(3), pp.291-300, (1988).

12. M. S. Dadkhah, A. S. Kobayashi, F. X. Wang, and D. L. Graesser, "J-Integral Measurement Using Moire Interferometry," Proceedings of the VI International Congress on Experimental Mechanics, Portland, OR, pp.227-234, (1988).

13. J.W. Hutchinson, "Singular Behavior at the End of a Tensile Crack in a Hardening Material," Journal of Mechanics and Physics of Solids, Vol.16, pp.13-31, (1968).

14. J. R. Rice and G. F. Rosegren, "Plane Strain Deformation near a Crack Tip in a Power-Law Hardening Material," Journal of Mechanics and Physics of Solids, Vol.16, pp.1-12, (1968).

15. M.S. Dadkhah, "Analysis of Ductile Fracture Under Biaxial Loading Using Moire Interferometry," Ph.D. dissertation, University of Washington, (1988).

16. J.W. Hutchinson and P.C. Paris, "Stability Analysis of J-Controlled Crack Growth," Elastic-Plastic Fracture, ASTM STP 668, American Society for Testing and Materials, Philadelphia, Pa., pp.37-64, (1979).

17. C.F. Shih and M.D. German, "Requirements for a One Parameter Characterization of Crack Tip Field by The HRR Singularity," International Journal of Fracture, 17(1), pp.27-43, (1981).

18. D. A. Davis, J. A. Joyce, and R. A. Hays, "Application of the J-Integral and the Modified J-Integral to Cases of Large Crack Extension and High Toughness Levels," ASTM, 21st National Symposium on Fracture Mechanics, Annapolis, MD, June (1988).

19. M.S. Dadkhah and A.S. Kobayashi, "Elastic-Plastic Analysis of Large Aluminum Cruciform Specimens," to be presented in 1989 SEM Spring Conference on Experimental Mechanics.

20. J.R. Rice, "Stresses Due to a Sharp Notch in a Work-Hardening Elastic-Plastic Material Loaded by Longitudial Shear," Journal of Applied Mechanics, Vol.34, pp.287-298, (1967).

21. J. C. Amazigo, "Some Mathematical Problems of Elastic-Plastic Crack Growth," Fracture Mechanics 12, SIAM-AMS Proceedings, R. Burridge Editor, pp.125, (1978).

Table 1 Test Material Properties

Aluminum	Yield Stress MPa (ksi)	Young's Modulus MPa (ksi)	α	n
2024-O	67 (9.7)	74200 (10760)	1.0	4
5052-H32	190 (27.6)	70000 (10150)	1.0	16

$$\frac{\varepsilon}{\varepsilon_y} = \frac{\sigma}{\sigma_y} + \alpha \left(\frac{\sigma}{\sigma_y} \right)^n$$

(Ramberg-Osgood Relation)

Table 2 Measured J-integral Values for Different Contours in a Uniaxially Loaded 5052-H32 Aluminum Single-edge Cracked, Cruciform Specimen

Applied Load (N)	Crack Extension (mm)	J^* (kPa-m) Contour # 1	J^* (kPa-m) Contour # 2	J^{**} (kPa-m) Contour # 1	J^{**} (kPa-m) Contour # 2	% Difference Contour # 1	% Difference Contour # 2
2371	0.0	4.80	5.20	4.22	4.35	12%	16%
3812	0.2	8.00	7.30	6.76	6.32	15%	13%
4404	0.36	12.10	11.60	12.50	12.30	3%	6%
5253	0.50	18.45	17.10	18.40	19.20	0.3%	12%
5760	0.75	23.81	25.29	23.40	23.62	2%	6%
6779	1.35	42.80	40.40	42.20	41.60	1%	3%
7455	1.95	66.70	64.70	66.60	61.20	0.2%	5%

* : Measured J values based on the exact J-evaluation procedure

** : Measured J values based on the approximate J-evaluation procedure

Table 3 Measured J-integral Values for Different Contours in a Uniaxially Loaded 2024-O Aluminum Single-edge Cracked, Cruciform Specimen

Applied Load (N)	Crack Extension (mm)	J^* (kPa-m) Contour # 1	J^* (kPa-m) Contour # 2	J^{**} (kPa-m) Contour # 1	J^{**} (kPa-m) Contour # 2	% Difference Contour # 1	% Difference Contour # 2
1019	0.0	0.25	0.26	0.21	0.22	16%	15%
1490	0.1	1.90	1.76	1.88	1.81	1%	3%
2576	0.33	6.30	6.70	6.20	6.30	2%	6%
3283	0.96	19.70	20.30	18.80	18.90	5%	7%
3763	1.34	31.00	28.50	31.70	30.10	2%	6%

* : Measured J values based on the exact J-evaluation procedure

** : Measured J values based on the approximate J-evaluation procedure

Table 4 Measured J-integral Values for Different Contours in a Biaxially Loaded 2024-O Aluminum Single-edge Cracked, Cruciform Specimen

Applied Load(Y) (N)	Applied Load(X) (N)	Crack Extension (mm)	J^* (kPa-m) Contour # 1	J^* (kPa-m) Contour # 2	J^{**} (kPa-m) Contour # 1	J^{**} (kPa-m) Contour # 2	% Difference Contour # 1	% Difference Contour # 2
4066	2086	0.04	4.00	3.80	3.26	3.08	19%	19%
5489	2896	0.50	11.00	10.50	9.25	9.11	16%	13%
5591	3305	0.85	18.10	18.40	14.30	14.70	21%	20%
5845	3888	1.34	31.00	29.00	25.70	24.36	17%	16%
6076	3914	1.40	32.00	29.20	26.00	25.10	19%	14%
6720	4524	1.68	34.00	31.00	28.50	28.00	16%	10%
6810	4626	2.20	50.00	47.00	40.50	39.80	19%	15%

* : Measured J values based on the exact J-evaluation procedure

** : Measured J values based on the approximate J-evaluation procedure

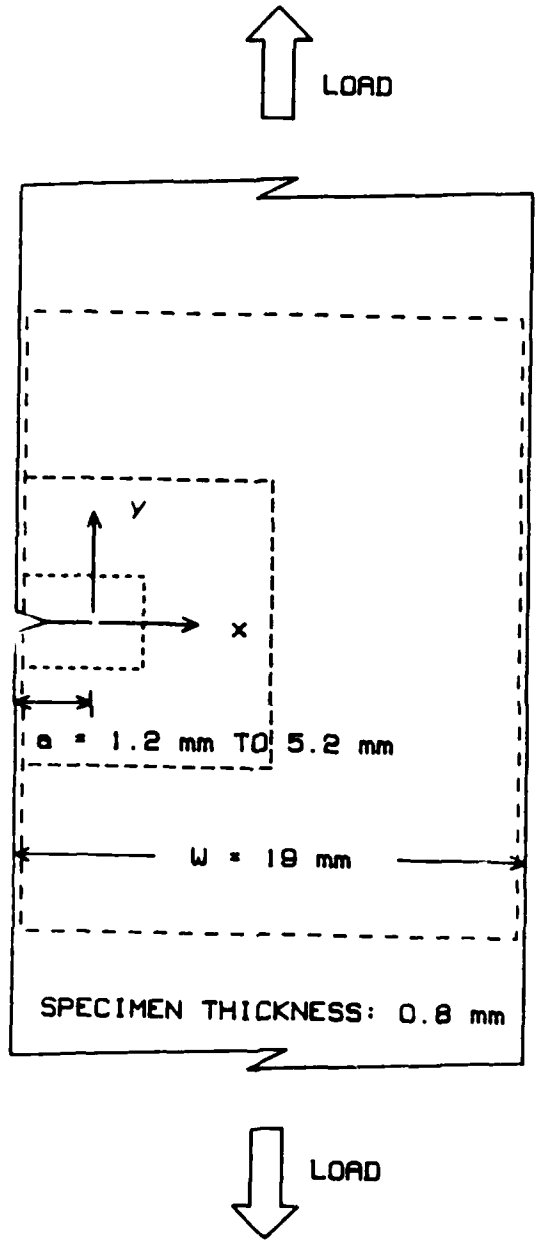

Fig. 1 Single Edge Notched (SEN) Specimen and Contours for J Evaluation.

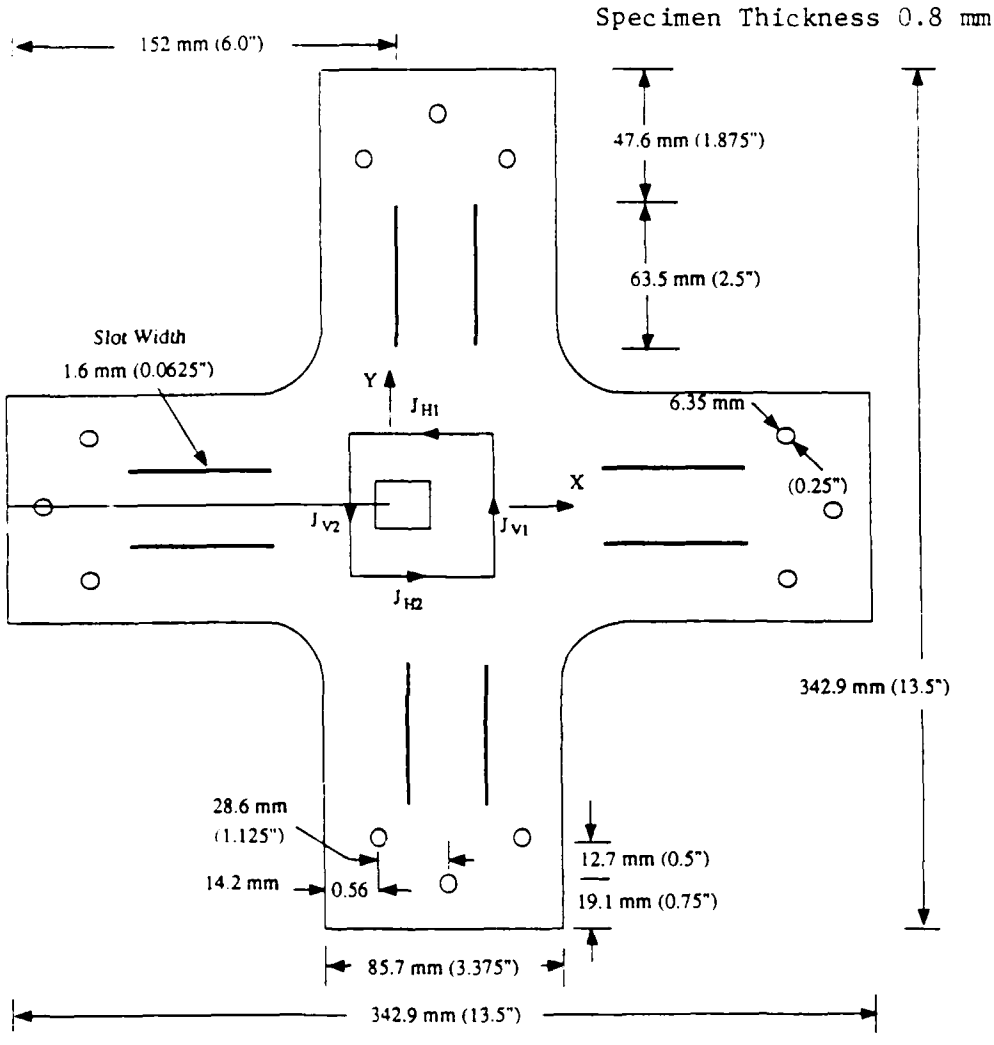

Fig. 2 Single Edge Cracked, Cruciform Specimen and Contours for J Evaluation.

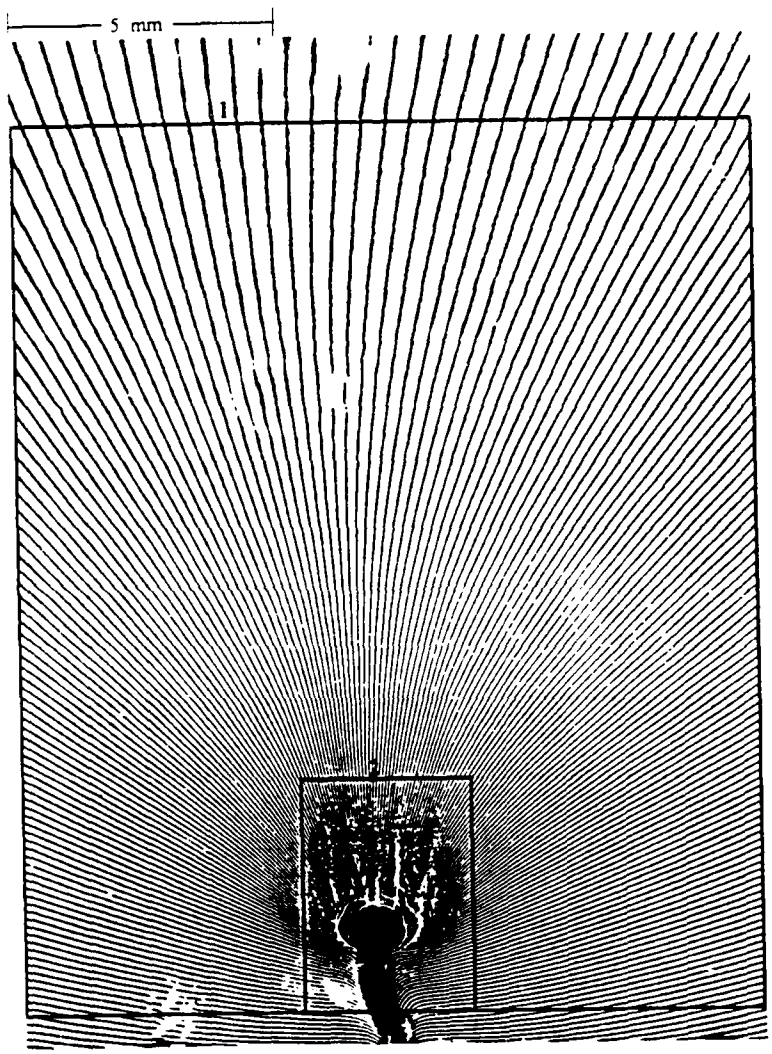

Fig. 3 u_y-Displacement in a Uniaxially Loaded 5052-H32 Aluminum Single Edge Cracked, Cruciform Specimen; Applied Load 5760 (N).

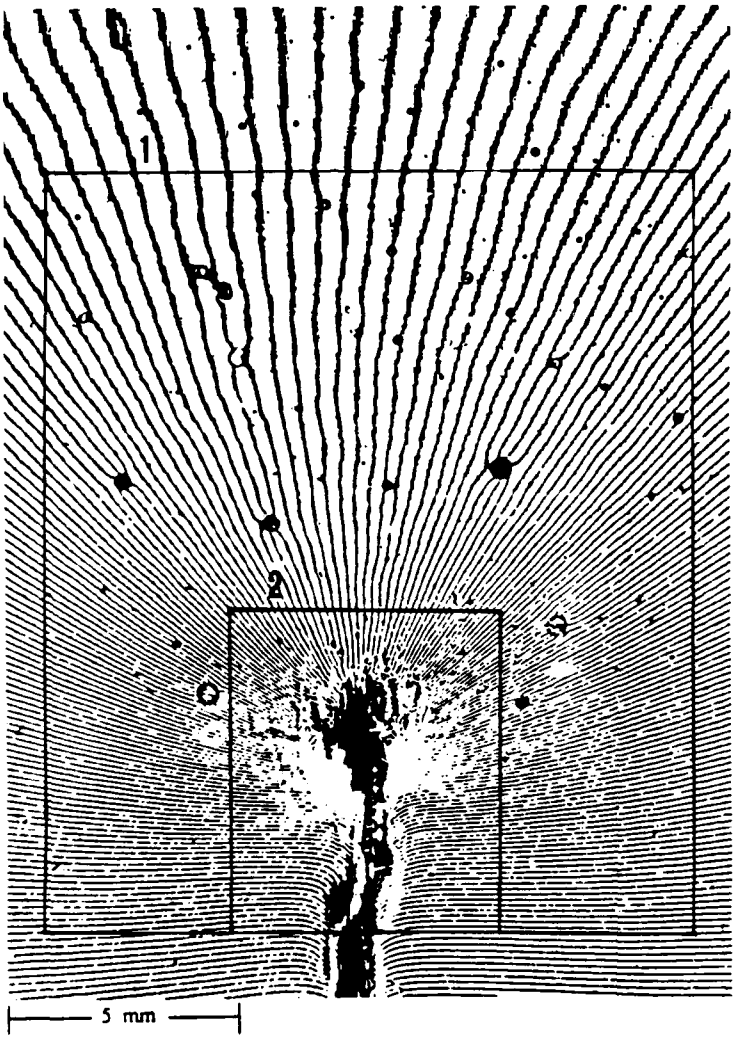

Fig. 4 u_y-Displacement in a Biaxially Loaded 2024-0 Aluminum Single Edge Cracked, Cruciform Specimen; Applied Load F_x = 5489 (N), F_y = 2896 (N).

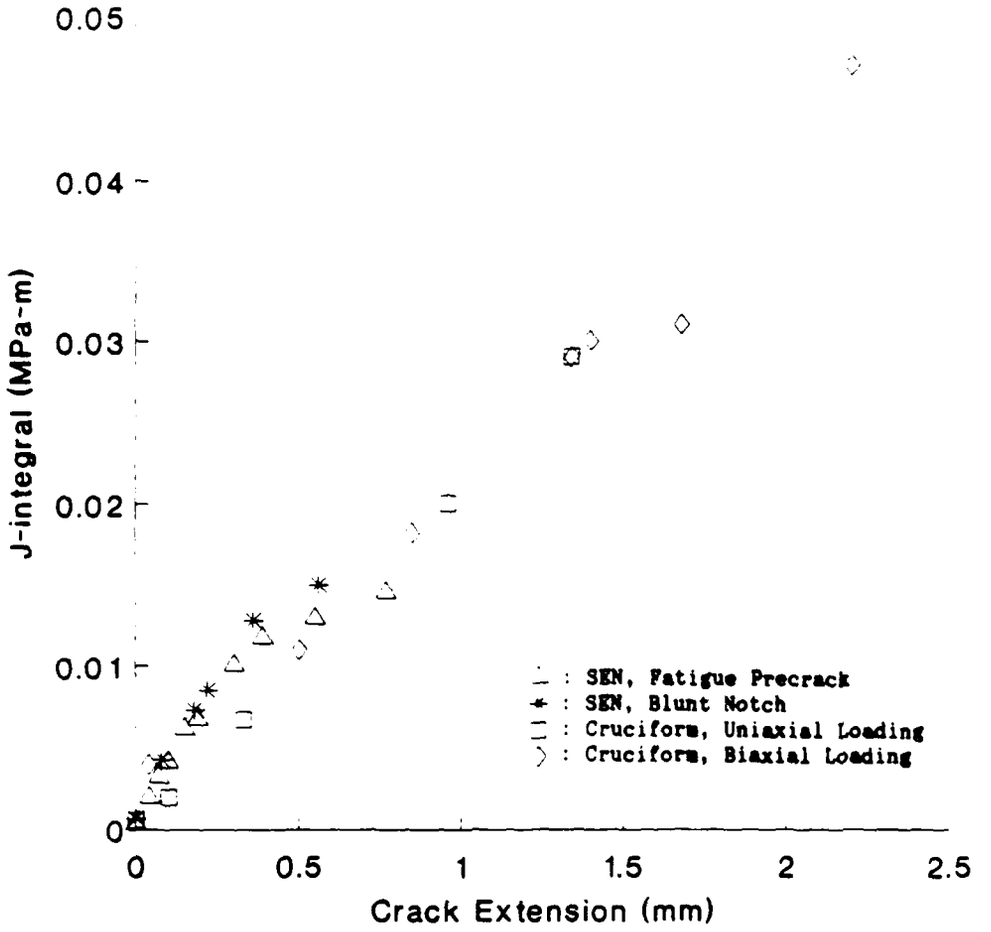

Fig. 5 J_R Curves of 2024-0 Aluminum Small SEN and Large Single Edge Cracked, Cruciform Specimens.

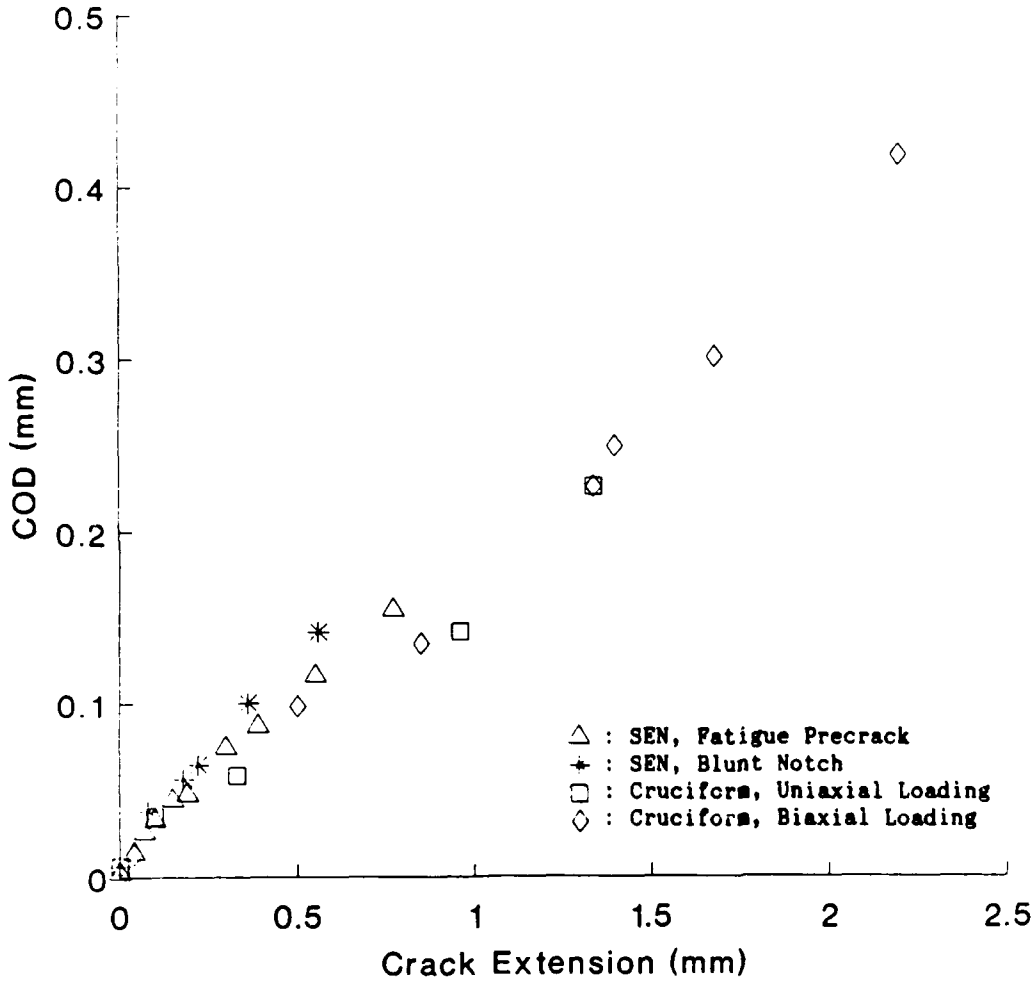

Fig. 6 COD Resistance Curves of 2024-0 Aluminum Small SEN and Large Single Edge Cracked, Cruciform Specimens.

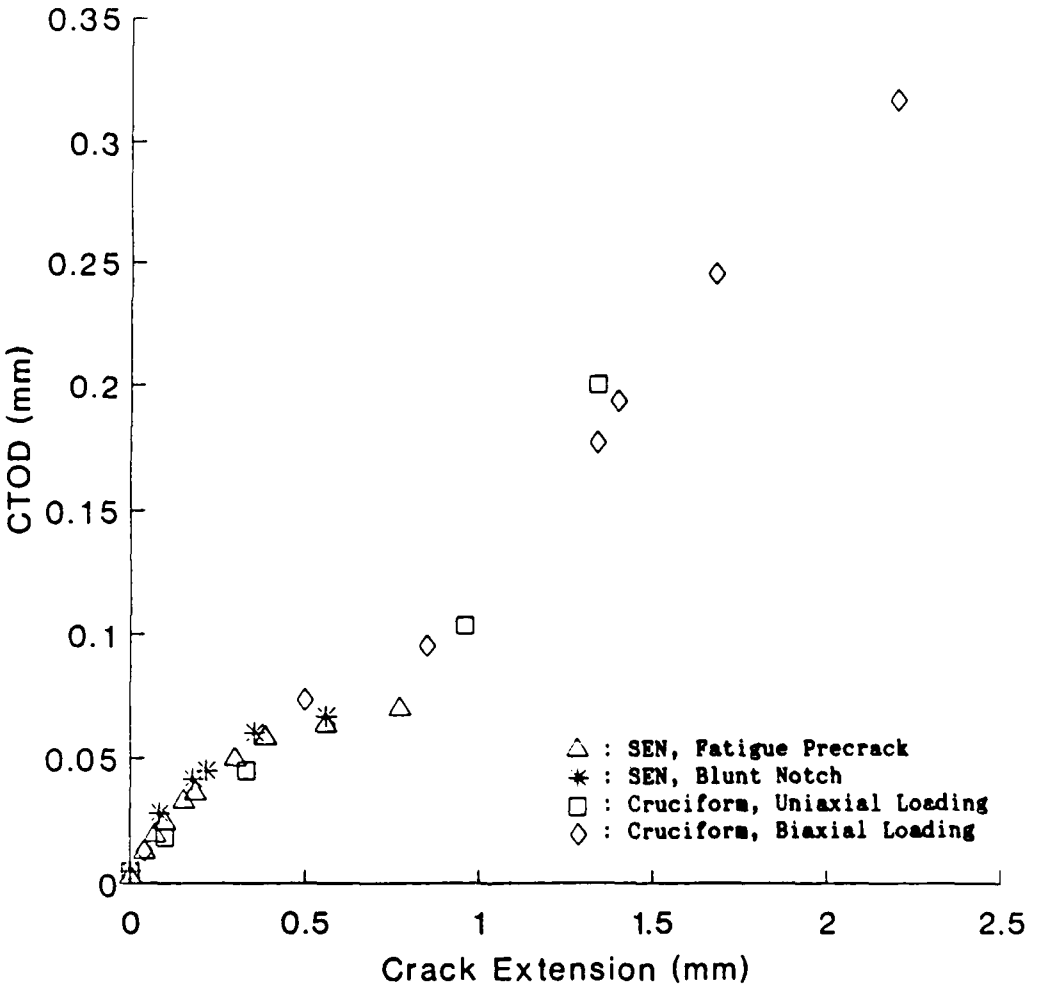

Fig. 7 CTOD Resistance Curves of 2024-0 Aluminum Small SEN and Large Single Edge Cracked, Cruciform Specimens.

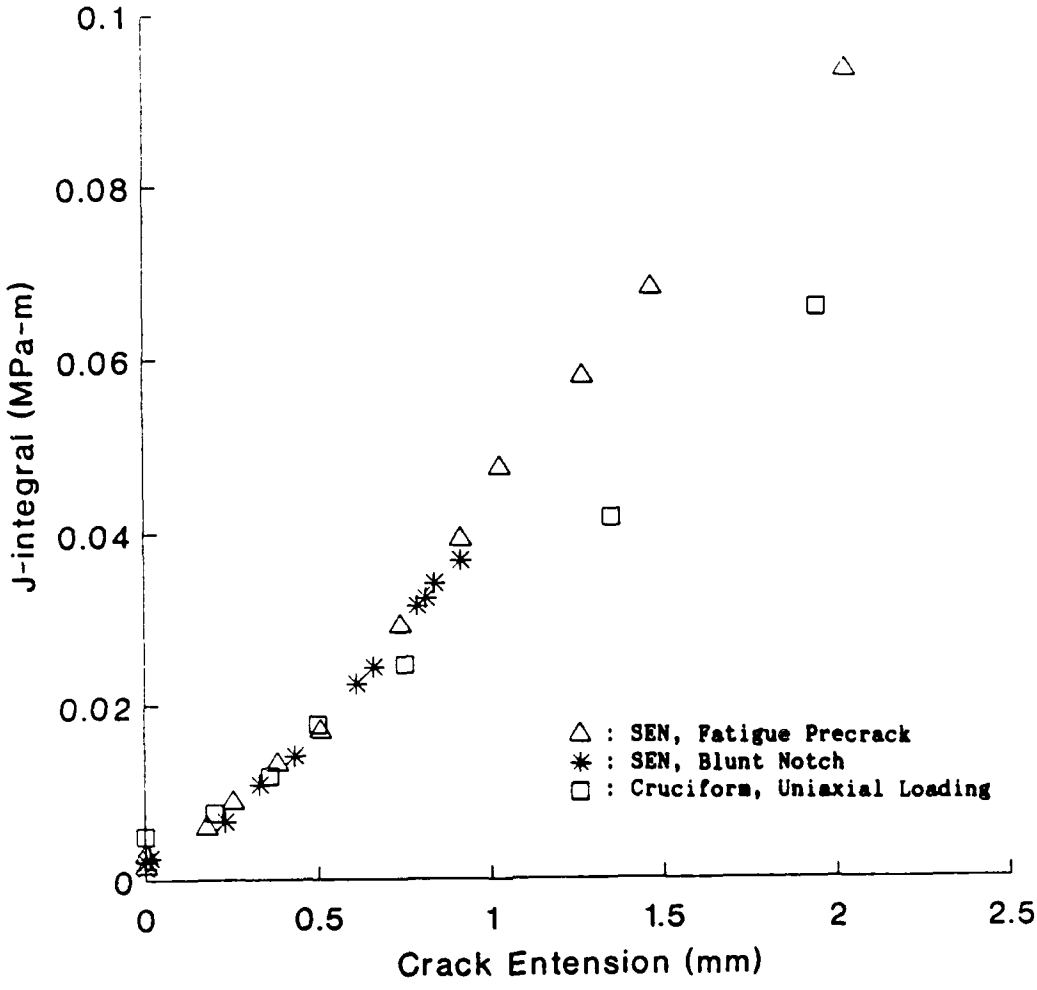

Fig. 8 J_R Curves of 5052-H32 Aluminum Small SEN and Large Single Edge Cracked, Cruciform Specimens.

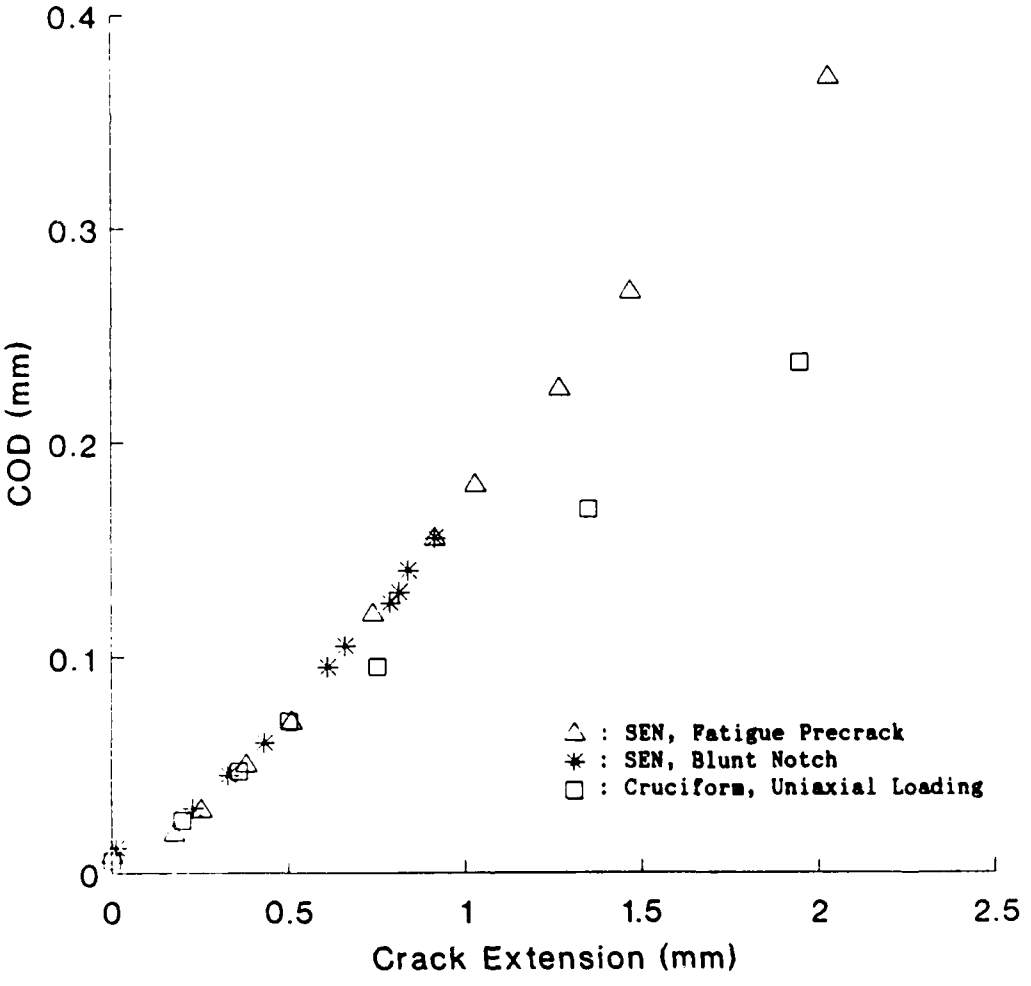

Fig. 9 COD Resistance Curves of 5052-H32 Aluminum Small SEN and Large Single Edge Cracked, Cruciform Specimens.

Office of Naval Research
800 N Quincy Street
Arlington, VA 22217-5000
Attn: Code 11325M (4 copies)

Office of Naval Research
800 N Quincy Street
Arlington, VA 22217-5000
Attn: Code 1131

Defense Documentation Cntr
(4 copies)
Cameron Station
Alexandria, VA 02314

Naval Research Laboratory
Washington, DC 20375
Attn: Code 6000

Naval Research Laboratory
Washington, DC 20375
Attn: Code 6300

Naval Research Laboratory
Washington, DC 20375
Attn: Code 6380

Naval Research Laboratory
Washington, DC 20375
Attn: Code 5830

Naval Research Laboratory
Washington, DC 20375
Attn: Code 6390

Naval Research Laboratory
Washington, DC 20375
Attn: Code 2620

David W. Taylor Naval Ship
R & D Center
Annapolis, MD 21402
Attn: Code 28

David W. Taylor Naval Ship
R & D Center
Annapolis, MD 21402
Attn: Code 2812

David W. Taylor Naval Ship
R & D Center
Annapolis, MD 21402
Attn: Code 2814

David W. Taylor Naval Ship
R & D Center
Annapolis, MD 21402
Attn: Code 1700

David W. Taylor Naval Ship
R & D Center
Annapolis, MD 21402
Attn: Code 1720

David W. Taylor Naval Ship
R & D Center
Annapolis, MD 21402
Attn: Code 1720.4

Naval Air Development
Center
Warminster, PA 18974
Attn: Code 6043

Naval Air Development
Center
Warminster, PA 18974
Attn: Code 6063

Naval Surface Weapons
Center
White Oak, MD 20910
Attn: Code R30
Technical Library

Naval Surface Weapons
Center
Dahlgren, VA 22448
Attn: Technical Library

Naval Civil Eng Library
Port Hueneme, CA 93043
Attn: Technical Library

Naval Underwater Systems
Center
New London, CT 06320
Attn: Code 44
Technical Library

Naval Underwater Systems
Center
Newport, RI 02841
Attn: Technical Library

Naval Weapons Center
China Lake, CA 99555
Attn: Technical Library

NRL/Underwater Sound
Reference Dept.
Orlando, FL 32856
Attn: Technical Library

Chief of Naval Operations
Department of the Navy
Washington, DC 20350
Attn: Code OP-098

Commander
Naval Sea Systems Command
Washington, DC 20362
Attn: Code 05R25

Commander
Naval Sea Systems Command
Washington, DC 20362
Attn: Code 05R26

Commander
Naval Sea Systems Command
Washington, DC 20362
Attn: Code 09B31

Commander
Naval Sea Systems Command
Washington, DC 20362
Attn: Code 55Y

Commander
Naval Sea Systems Command
Washington, DC 20362
Attn: Code 55Y2

Commander
Naval Sea Systems Command
Washington, DC 20362
Attn: Code 03D

Commander
Naval Sea Systems Command
Washington, DC 20362
Attn: Code 7226

Commander
Naval Sea Systems Command
Washington, DC 20362
Attn: Code 310A

Commander
Naval Sea Systems Command
Washington, DC 20362
Attn: Code 310B

US Naval Academy
Mechanical Engineering Dept.
Annapolis, MD 21402

Naval Postgraduate School
Monterey, CA 93940
Attn: Technical Library

Mr. Jerome Persh
Stf Speclt for Matls &Struct
OUSDE & E. The Pentagon
Room 301089
Washington, DC 20301

Professor J. Hutchinson
Harvard University
Div. of Applied Sciences
Cambridge, MA 02138

Dr. Harold Liebowitz, Dean
School of Engr. & Applied Sci.
George Washington
University
Washington, DC 20052

Professor G.T. Hahn
Vanderbilt University
Dept. of Mech. & Matrls. Engr.
Nashville, TN 37235

Professor Albert S.
Kobayashi
Dept. of Mechanical
Engineering
University of Washington
Seattle, WA 98195

Professor L.B. Freund
Brown University
Division of Engineering
Providence, RI 02912

Professor B. Budiansky
Harvard University
Division of Applied Sciences
Cambridge, MA 02138

Professor S.N. Atluri
Georgia Institute of
Technology
School of Engr. & Mechanics
Atlanta, GA 30332

Professor G.Springer
Stanford University
Dept. of Aeronautics
& Astronautics
Stanford, CA 94305

Professor H.T. Hahn
Dept of Engr Sciences &
Mech
Penn State University
227 Hammond Bldg
University Park, PA 16802

Professor S.K. Datta
University of Colorado
Dept. of Mechanical
Engineering
Boulder, CO 80309

Dr. M.L. Williams
School of Engineering
University of Pittsburgh
Pittsburgh, PA 15261

Professor R.H. Gallagher
President
Clarkson University
Potsdam, NY 13676

Dr. D.C. Drucker
Dept. of Aerospace Eng.
& Mechanics
University of Florida
Tallahassee, FL 32611

Professor B.A. Boley
Dept. of Civil Engineering
Columbia University
New York, NY 10025

Professor J. Duffy
Brown University
Division of Engineering
Providence, RI 02912

Professor J.D. Achenbach
Northwestern University
Dept of Civil Engineering
Evanston, IL 60208

Professor F.A. McClintock
Dept of Mechanical
Engineering
Massachusetts Institute of
Technology
Cambridge, MA 02139

Professor D.M. Parks
Dept of Mechanical
Engineering
Massachusetts Institute of
Technology
Cambridge, MA 02139

Dr. M.F. Kanninen
Southwest Research
Institute
PO Drawer 28510
6220 Culebra Road
San Antonio, TX 78284

Professor F.P. Chiang
Dept of Mechanical Engr
State U of NY at Stony Brook
Stony Brook, NY 11794

Professor S.S. Wang
Dept of Theoretical & Appl
Mechs
University of Illinois
Urbana, IL 61801

Professor Y. Weitsman
Civil Engr Department
Texas A&M University
College Station, TX 77843

Professor I.M. Daniel
Dept of Mechanical Engr
Northwestern University
Evanston, IL 60208

Professor C.T. Sun
School of Aeronautics
& Astronautics
Purdue University
W. Lafayette, IN 47907

Professor J. Awerbuch
Dept of Mech Engr &
Mechanics
Drexel University
Philadelphia, PA 19104

Professor T.H. Lin
University of California
Civil Engineering Dept
Los Angeles, CA 90024

Professor G.J. Dvorak
Dept of Civil Engr
Rensselaer Polytecnic
Institute
Troy, NY 12180

Dr. R.M. Christensen
Chemistry & Mtrl Sci Dept
Lawrence Livermore Natl
Lab
PO Box 80P
Livermore, CA 94550

Professor J.R. Rice
Division of Applied Sciences
Harvard University
Cambridge, MA 02138

Professor W.N. Sharpe
The Johns Hopkins
University
Dept of Mechanics
Baltimore, MD 21218

Professor C.F. Shih
Brown University
Division of Engineering
Providence, RI 02912

Professor A. Rosakis
California Institute of Tech
Graduate Aeronautical Labs
Pasadena, CA 91125

Professor D. Post
VA Polytechnic & State U
Dept of Engr Science &
Mechanics
Blacksburg, VA 24061

Professor W. Sachse
Cornell University
Dept of Theoretical &
Applied Mechanics
Ithaca, NY 14853

Unclassified

SECURITY CLASSIFICATION OF THIS PAGE (When Data Entered)

REPORT DOCUMENTATION PAGE		READ INSTRUCTIONS BEFORE COMPLETING FORM
1. REPORT NUMBER UWA/DME/TR-89/62	2. GOVT ACCESSION NO.	3. RECIPIENT'S CATALOG NUMBER
4. TITLE (and Subtitle) J-Resistance Curves of Aluminum Specimens Using Moire Interferometry		5. TYPE OF REPORT & PERIOD COVERED 6. PERFORMING ORG. REPORT NUMBER UWA/DME/RT-89/62
7. AUTHOR(s) B.S.-J. Kang, M.S. Dadkhah and A.S. Kobayashi		8. CONTRACT OR GRANT NUMBER(s) N00014-89-J-1276
9. PERFORMING ORGANIZATION NAME AND ADDRESS Department of Mechanical Engineering, FU-10 University of Washington Seattle, Washington 98195		10. PROGRAM ELEMENT, PROJECT, TASK AREA & WORK UNIT NUMBERS
11. CONTROLLING OFFICE NAME AND ADDRESS Office of Naval Research Arlington, Virginia 22217		12. REPORT DATE April 1989 13. NUMBER OF PAGES 18
14. MONITORING AGENCY NAME & ADDRESS(if different from Controlling Office)		15. SECURITY CLASS. (of this report) Unclassified 15a. DECLASSIFICATION/DOWNGRADING SCHEDULE

16. DISTRIBUTION STATEMENT (of this Report)

Unlimited

17. DISTRIBUTION STATEMENT (of the abstract entered in Block 20, if different from Report)

18. SUPPLEMENTARY NOTES

19. KEY WORDS (Continue on reverse side if necessary and identify by block number)

Moire Interferometry, Elastic-plastic Fracture Mechanics, J-Resistance Curve

20. ABSTRACT (Continue on reverse side if necessary and identify by block number)

Errors involved in using the approximate J-evaluation procedure are evaluated by comparing the resistance curves of large 2024-0 and 5052-H32 aluminum, single-edge cracked, cruciform specimens under uniaxial and biaxial loadings with those obtained by an exact procedure. This comparative study shows that under uniaxial loading, the J-resistance curves obtained by the approximate procedure are within six percent of those obtained by the exact procedure. For the biaxial loading, however, the difference is about eighteen percent.

(over)

DD FORM 1 JAN 73 1473 EDITION OF 1 NOV 65 IS OBSOLETE
S/N 0102-014-6601

Unclassified

SECURITY CLASSIFICATION OF THIS PAGE (When Data Entered)

20. Abstract (continued).

The specimen size and geometry dependence of the J-resistance curves of 2024-0 and 5052-H32 aluminum specimens are also discussed.